Upgrading of raw biogas using membranes based on the ultrapermeable polymer of intrinsic microporosity PIM-TMN-Trip

Upgrading of raw biogas using membranes based on the ultrapermeable polymer of intrinsic microporosity PIM-TMN-Trip

Petr Stanovsky[1,2], Magda Kárászova[1], Zuzana Petrusova[1], Marcello Monteleone[3], Johannes Carolus Jansen[3,*], Bibiana Comesaña Gándara[4], Neil B. McKeown[4], Pavel Izak[1,2,5,*]

[1] The Czech Academy of Sciences, Institute of Chemical Process Fundamentals, Rozvojova 135, 165 02 Prague 6 – Suchdol, Czech Republic

[2] Institute of Environmental Technology VSB-TUO, 17. listopadu 15/2172, 708 33 Ostrava-Poruba, Czech Republic

[3] Institute on Membrane Technology, CNR-ITM, Via P. Bucci 17/C, 87036 Rende (CS), Italy

[4] EaStCHEM School of Chemistry, University of Edinburgh, David Brewster Road, Edinburgh EH9 3FJ, Midlothian, Scotland

[5] MemBrain s.r.o., Pod Vinicí 87, 471 27 Stráž pod Ralskem, Czech Republic

* corresponding author: izak@icpf.cas.cz, johannescarolus.jansen@cnr.it

Abstract

The potential of an ultrapermeable benzotriptycene-based polymer of intrinsic microporosity (PIM-TMN-Trip) for the upgrading of biogas is investigated. Permeation experiments were performed using an in-house bespoke permeation unit for pure gases and gas mixtures, and included tests with model mixtures as well as real biogas from a sewage treatment plant, under dry and humid conditions. Permeability and CO_2/CH_4 selectivity for either pure gases or for real biogas were high and lie close to or on the recently defined 2019 Robeson upper bound based on ideal permselectivities. In addition, a remarkable increase in CO_2/CH_4 selectivity was observed after two weeks of continuous exposure to CO_2 due to a significant decrease of CH_4 permeability. The constant CO_2 permeability and increased selectivity upon ageing suggest that ageing in the presence of CO_2 causes a rearrangement, rather than a reduction of the fractional free volume. The mixed gas permeability experiments were performed with high stage-cut in order to mimic a real separation process, and the results confirmed the potential of PIM-TMN-Trip membranes for biogas upgrading.

Keywords

biogas upgrading; gas permeation; polymer of intrinsic microporosity; membrane gas separation

1 Introduction

The need for sustainable, environmentally friendly and renewable energy is resulting in a gradual shift towards energy production using renewable sources, including biomass [1-6]. Biogas is one of the most common and readily available renewable energy sources. It is a product of an anaerobic digestion of organic waste and it contains 50-70 vol% of CH_4 with the remainder mostly CO_2, water vapour up to saturation and trace amounts of other organic gas by-products [7]. Upgrading of biogas streams focuses on obtaining a product with a higher calorific value to avoid the meaningless heating of the inert components and problems with component corrosion from moist CO_2. In addition, in order to become compatible and competitive with natural gas, biogas must meet the specifications of grid-quality methane. Therefore, CO_2 separation from biogas is becoming an increasingly important field, where membrane separations are proven as a successful technology. However, despite their success on an industrially relevant scale [1, 8], there is still a strong need to improve the energy efficiency of membranes [9], and to provide more permeable polymer materials for CO_2/CH_4 separation membranes to make this technology more profitable and economically competitive [10, 11]. This challenge has been addressed by the development of novel materials to make membranes for biogas separation [12], based on novel polymers and on mixed matrix membranes [5, 13].

Polymers of Intrinsic Microporosity (PIMs) are promising membrane materials showing extremely high CO_2 permeability and good CO_2/CH_4 selectivity. This class of polymer has is composed of a highly rigid backbone and monomeric units, composed of a site of contortion (e.g. spiro-centre or bridged bicyclic unit), which are responsible for generating microporosity leading to high gas and vapour solubility. They offer the key advantage of solubility in common organic solvents, hence thin film composite membranes relevant for industial use can be easily prepared by solution casting [14-17]. In particular, PIMs derived from exceptionally rigid components such as triptycene, spirobifluorene or Tröger's base possess excellent separation properties [18-22]. In addition, various copolymers can be made, some of which show promising results for gas permeability and selectivity [23]. The structural diversity of PIMs can be increased by the choice of the monomer [24-26] or by introducing functional groups to modify gas selectivity [27, 28]. Recently, ultrapermeable benzotriptycene-derived PIMs, based on two-dimensional chains that pack inefficiently, were used to re-define the Robeson upper bound for CO_2/CH_4 and CO_2/N_2 based on their single gas permeabilities [29].

The objective of the present study was to prove the practical applicability of this new membrane material, not only with model mixtures but also with real, industrially relevant gas streams. Such studies are extremely rare for PIMs with, to our knowledge, only the CO_2 capture from a real flue gas stream by PIM-1 [30] or by PIM-TMN-Trip [31], the polymer used in the present study, being reported. Here, the transport and separation properties of PIM-TMN-Trip [21], were studied with both pure gas streams (CH_4 and CO_2) and mixed gas streams based on either model binary mixtures or on raw biogas. Moreover, the influence of the trans-membrane pressure difference, and the influence of prolonged membrane exposure to CO_2 was also determined.

2 Experimental and methodology

2.1 Materials and membrane preparation

Membranes were prepared as freestanding films by casting chloroform solutions of the polymer PIM-TMN-Trip (Fig. 1) in a Petri dish, followed by slow evaporation of the solvent and further treatment of the membrane with methanol to remove residual casting solvent. The preparation procedure of the membrane is described in detail by Rose *et al*. [21].

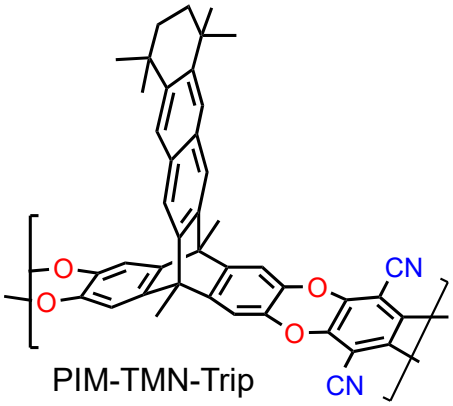

Fig. 1. The molecular structure of PIM-TMN-Trip.

The permeability was tested with pure gases (CO_2, CH_4, N_2) with a nominal purity of 99.95% or higher. All gases were purchased from Linde Gas. The biogas used in this study was obtained from the Prague Central Wastewater Treatment Plant directly from the line after the pre-drying section to prevent condensation of humidity inside the cylinder. The biogas was collected before the cleaning unit containing activated carbon, so that our testing biogas mixture contains, besides common CO_2 and CH_4, also nitrogen (N_2) hydrogen sulphide (H_2S) and traces of various other compounds that may be present in biogas, such as siloxanes and volatile organic compounds (VOCs) [1, 11, 32].

2.2 Experimental apparatus

The gas permeation experiments of selected gases and gas mixtures were carried out with a circular membrane with an effective area of 15.91 cm^2, placed on a porous stainless-steel support, and sealed by an O-ring in the permeation cell. The permeation cell was designed and assembled at ICPF CAS, and the radial flow profiles at the feed side and the permeate side can be operated both in co-current mode or in counter-current mode (this work). A continuous flow system is controlled via National Instruments analogue/digital I/O boards and operated via routines programmed in LabVIEW. The tested membranes (Fig. 2) had an average thickness of 161 ± 13 μm determined by a digital micrometre Micromaster® Capaμsystem IP54 (Switzerland).

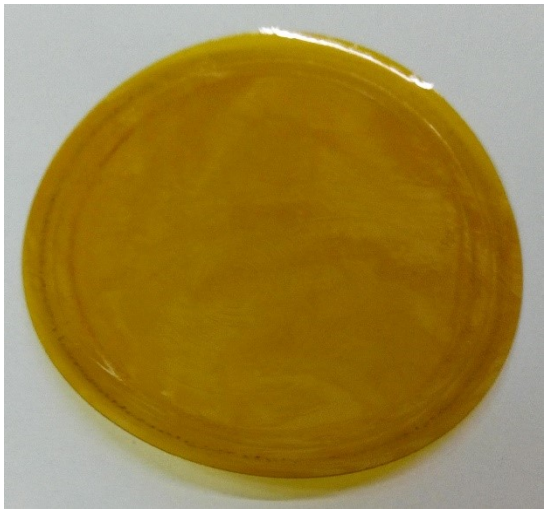

Fig. 2. PIM-TMN-Trip membrane after the permeation tests, showing no visible change compared to the original membrane.

The permeation apparatus, schematically depicted in Fig. 3, allows the study of either pure gas (CH_4 or CO_2), model mixtures of CH_4 with CO_2, or a feed stream of real biogas, collected in a gas cylinder at the sewage plant in Prague. The raw biogas was already pre-dried because it is the easiest stream that can be collected at the sewage plant, and it was compressed into a gas cylinder up to 500 kPa. A set of mass flow controllers (Bronkhorst, range 3-100 ml min^{-1}) control the flow rate of feed and N_2 sweep stream, respectively.

The permeation apparatus is equipped with humidifiers and sensors to control and measure the relative humidity of the feed and permeate streams, but in this work the experiments were conducted only with dry gases and gas mixtures to avoid the membrane swelling caused by the humidity. Only the raw biogas used in this work was slightly humid – dew point about 10 °C.

Two backward-operating pressure regulators (Bronkhorst, El-flow P702CV) control the pressure in the two branches of the permeation apparatus. (feed side of the cell in the range 100-500kPa, permeate side in the range 20-100kPa). The flow rates of both output streams (retentate and permeate) are analysed with mass flow gauges (Bronkhorst, range 1-30 ml min^{-1}), followed by a cold trap, working at the temperature of -4 °C, reducing the water vapour pressure before the gas analyser to values lower than 0.45 kPa to avoid humidity in the gas analyser.

The composition of the permeate and retentate streams, as well as that of the feed stream via a bypass, were determined with the biogas analyser (ASEKO AIR LF), using electrochemical sensors (for O_2, H_2S) and infrared sensors (for CO_2 and CH_4). The analyser is calibrated by certified laboratory and the analyse is periodically check by the model binary mixtures with known compositions.

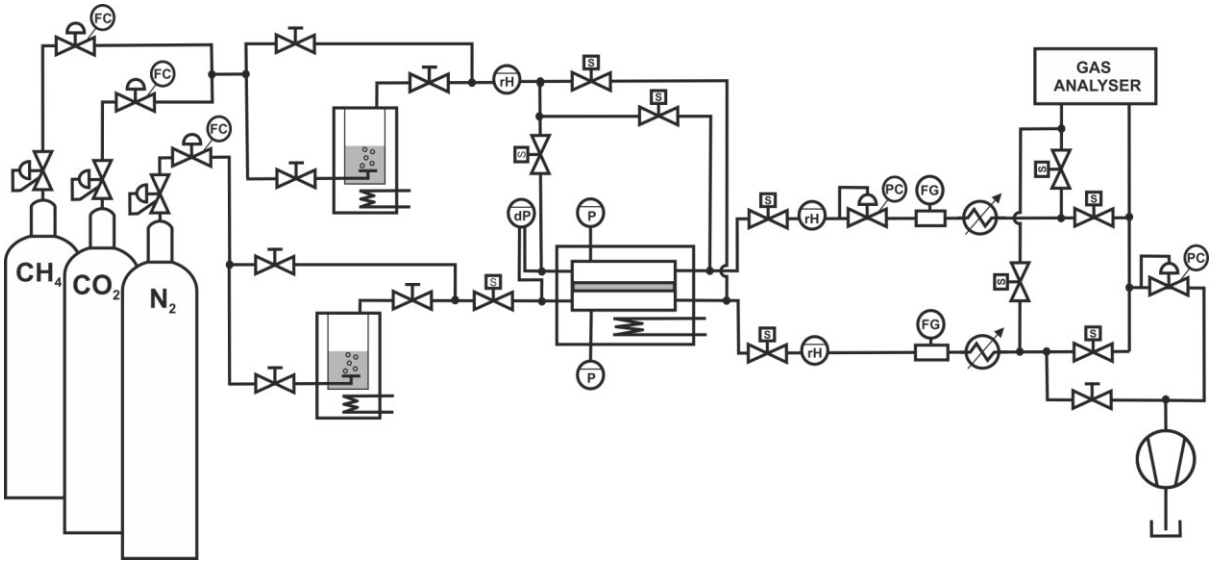

Fig. 3. Scheme of CO_2/CH_4 permeation apparatus with humidity control. FC – flow controllers, P – pressure gauges, dP – pressure difference gauge, FG – flow gauges, rH– humidity gauges, PC – pressure controllers, S – electromagnetic valves.

Permeation measurements were carried out at 25 °C with an upstream pressure ranging from 100 kPa to 500 kPa and at a constant downstream pressure of 100 kPa. The total feed flow rate was 20.3 cm^3 min^{-1} and the N_2 sweep gas flow rate was 21.9 cm^3 min^{-1}. The permeability of pure gases and their mixtures was measured in the following order: pure CH_4, model binary mixture (containing 40 vol.% CO_2 and 60 vol.% CH_4), raw biogas collected at the Prague Central Wastewater Treatment Plant (containing 33.6 vol.% CO_2, 64.0 vol.% CH_4, 2.4 vol.% N_2 and 427 ppm H_2S), and finally pure CO_2. This specific test sequence was chosen to minimize the potential effect of changes in the membrane induced by sorption and desorption of CO_2 into and from the polymer. Subsequently, the transport and separation properties were studied after two weeks exposure of the membrane to CO_2 at 25 °C and at 500 kPa. The measurements of pure CO_2 and pure CH_4 were then repeated with smaller pressure increments within the whole range of upstream pressures. The order of experiments and their conditions are summarised in Table S1.

2.3 Calculations

The permeability was evaluated according to the following relation

$$P_i = \frac{J_i\, l}{\Delta p_m}, \qquad \text{Eq. 1}$$

where J_i is the permeation flux of a particular gas through the membrane, l is the thickness of the membrane and Δp_m is the driving force. The streams in the membrane cell flow in the counter-current arrangement. Therefore, the logarithmic average of the partial pressure differences of the respective streams is used and the driving force is calculated according to the following formula

$$\Delta p_m = \frac{(p_i^{feed} - p_i^{perm}) - (p_i^{ret} - p_i^{sweep})}{\ln(p_i^{feed} - p_i^{perm}) - \ln(p_i^{ret} - p_i^{sweep})}, \quad \text{Eq. 2}$$

The selectivity was calculated as the ratio of the permeabilities

$$\alpha_{i/j} = \frac{P_i}{P_j}, \quad \text{Eq. 3}$$

where P is expressed in the unit Barrer, recalculated from SI units, as: $1\ \text{Barrer} = 3.35 \times 10^{-16}\ \frac{\text{mol}}{\text{m.s.Pa}}$. The ideal selectivity is calculated from the permeabilities obtained from the measurements with pure gases, while the real selectivity (or mixed gas selectivity) is calculated from the permeabilities obtained from the study of a binary model mixture or a real multi-component mixture.

The transport properties can be determined by the parameter of stage-cut θ_i which is usually used for high permeable membranes. The stage-cut is defined as the percentage of a particular component in the feed stream, which permeates through the membrane:

$$\theta \text{i} = \frac{J_i^{membrane}}{x_i^{feed}\, Q^{feed}}, \quad \text{Eq. 4}$$

where J_i^{membrane} is the flux of i-th component through membrane and the quantity of this component in the feed stream is expressed by ($x_{i,}^{\text{feed}} \cdot Q^{\text{feed}}$), in which $x_{i,}^{\text{feed}}$ is the volume fraction of component i in the feed stream, and Q^{feed} is the total feed flow rate. The total stage-cut is then expressed as the ration between the total permeate flow (Q^{perm}) and the feed flow:

$$\theta_{\text{total}} = \frac{Q^{perm}}{Q^{feed}} = \frac{\sum_{i=1}^{N} J_i^{membrane}}{Q^{feed}}, \quad \text{Eq. 5}$$

where permeate flow is the sum of all permeating components and N represents the number of the components.

3 Results and discussion

3.1 Pure versus mixed gas permeation

Firstly, the PIM-TMN-Trip membrane was tested for the permeability of pure CH_4. Secondly, a binary model mixture (40/60 Vol.% CO_2/CH_4), and then real biogas were tested. The binary mixture contained 40 vol.% CO_2 and 60 vol.% CH_4, and real biogas, collected from Prague Central Wastewater Treatment Plant, contained 33.6 vol.% CO_2, 64.0 vol.% CH_4, 2.4 vol.% N_2 and 427 ppm H_2S. Finally, the permeability of pure CO_2 was measured. The membrane showed excellent separation performance for the CO_2/CH_4 mixture and high ideal selectivity for the pure gas measurements (Tab. S1 and Tab. S2 in the Supplementary information). The combination of separation and transport parameters for biogas and for CO_2/CH_4 (40:60) gas mixture lie above Robeson's upper bound for ideal selectivity from 2008 [33] and close to or on the proposed 2019 upper bounds for pure [29] and mixed gases [24] at low pressure (Fig. 4), although the selectivity reduces as the pressure is increased (Tab. S3 in the SI). For the same reason, the mixed gas permeation of the membrane is higher than the mixed gas upper bound for experiments at 20 bar proposed by Wang et al. [24], drawn also in Fig.4. The differences are caused partially due to the higher gas pressure, relevant to natural gas processing, for which this upper bound was determined [24]. Decrease of selectivity with increasing pressure for

mixed gas and biogas can be attributed to CO_2-induced alteration of the selective diffusion domains as was reported for other PIMs [34]. This is typical for all glassy polymers, in particular those with high free volume, and is also related to the dual mode sorption behaviour. Increasing pressure causes a gradually higher occupation of the Langmuir sorption sites, and thus a decrease in solubility [35].

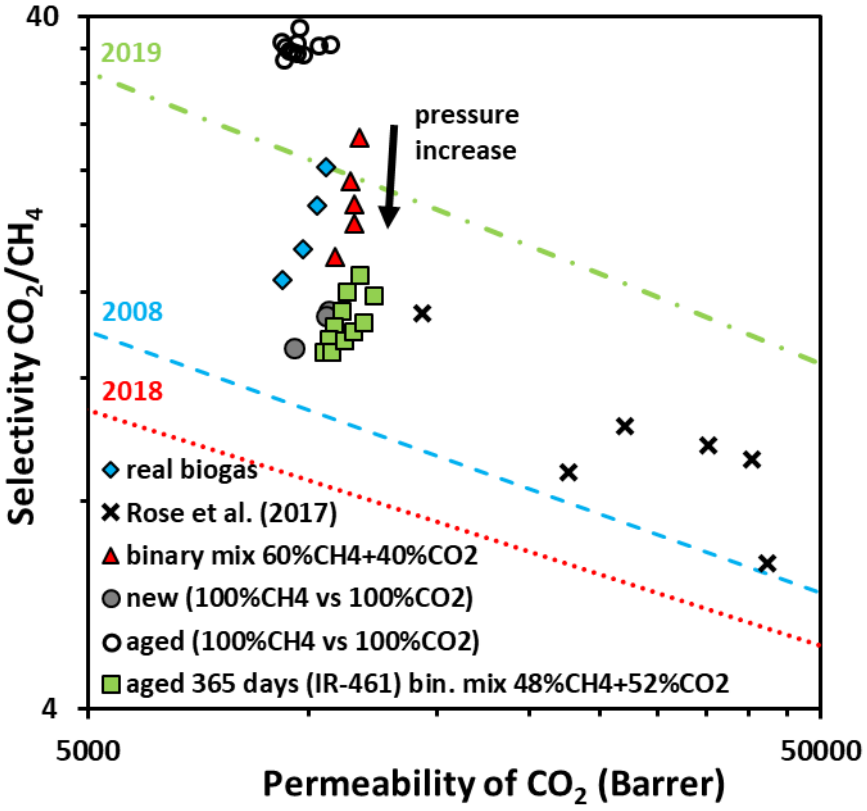

Fig. 4. Robeson diagram for CO_2/CH_4 with results for the PIM-TMN-Trip membrane for pure gases and for gas mixtures. Lines are upper bounds for separation of CO_2/CH_4 from literature for ideal selectivity: blue dashed line – Robeson *et al*. [33] green dash-dotted line – Comesaña-Gándara *et al*. [29]; and for mixed gas selectivity at high pressure (20 bar): red dotted line – Wang *et al*. [24]. Gases measured in the order 1) pure CH_4, 2) binary mixture, 3) real biogas, 4) pure CO_2, 5) pure CO_2, aged after CO_2 exposure, 6) pure CH_4 (all experimental conditions are summarised in Table S1). Green squares: control measurements on a different instrument (see Supporting Information)

The permeability and mixed gas selectivity for CO_2/CH_4 mixtures and real biogas as a function of pressure difference across the PIM-TMN-Trip membrane is shown in Fig. 5. There is almost negligible difference between the results from the mixture of 40 vol% CO_2 with 60 vol% CH_4 and those from real biogas (Tab. S3 and Tab. S4 in the SI). Despite the concentration of H_2S in the biogas being ~430 ppm, no H_2S-induced swelling was observed, even though some common membranes are susceptible to this effect at comparable H_2S concentration, and no reduction of permeability of other gases in the mixture was observed due to competitive

sorption at low partial pressures of H_2S [36-38]. This can be attributed to the high free volume and the resulting high sorption capacity of the membrane. [21] In addition, the lower concentration of H_2S, by two orders of magnitude as compared to that of CO_2, means that if most of the H_2S is adsorbed on the membranes there is still enough space for CO_2, reducing the effect of potential competition. The increase of CH_4 permeability at higher trans-membrane pressure, accompanied by a decrease of CO_2 permeability can be attributed to a coupling effect due to sorption nonideality [39] and, in part it could also be a result of concentration polarization phenomena.

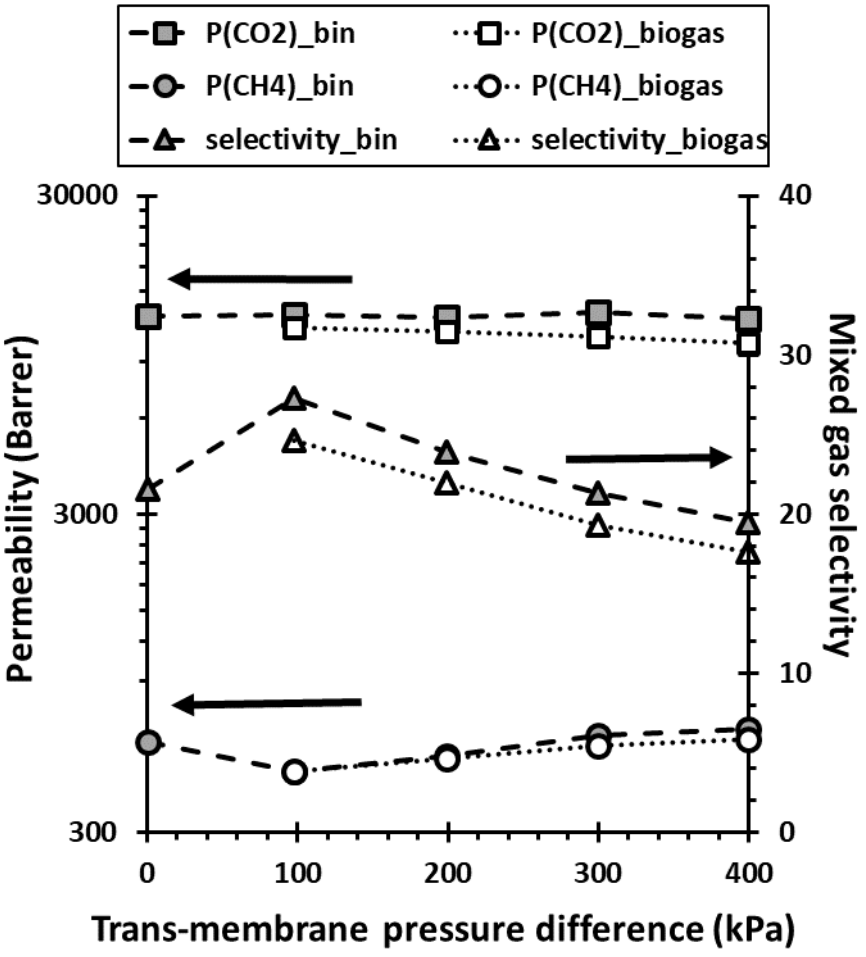

Fig. 5. Mixed gas permeability and selectivity for binary mixture of 40 vol% CO_2 and 60 vol% CH_4 (indicated as 'bin'), and for real biogas.

To verify whether concentration polarization may indeed be relevant, a simple calculation was performed for our permeation cell [40-44]. The circular membrane was placed in the cell with feed inflow above its centre and retentate outflows on the peripheral membrane edges. The sweep flow was set in the opposite direction, with the permeate flowing out from the cell centre, thus in counter-current mode. The space above the membrane, *h*, is 1 mm and the radial flow

in the cell can be described using Reynolds number *Re* changing with membrane radius. For the feed and sweep flow rate, calculations reveal that *Re* ranges from 7 down to 0.2. Therefore, a laminar flow profile exists in the cell on both sides. The thickness of the boundary layer across the cell increases up to a maximum of 6.5% of the cell height above membrane, according to the boundary layer theory [45]. The limitation of the driving force can be characterized by concentration polarization modulus M:

$$M = \frac{\exp(Pe)}{R_i + (1-R_i)\exp(Pe)} \quad \text{Eq.5}$$

evaluated from rejection factor *R*

$$R_i = 1 - \frac{p_i^{perm}}{p_i^{ret}} \quad \text{Eq.6}$$

and Peclet number *Pe*

$$Pe = \frac{J_i}{k_i} \quad \text{Eq.7}$$

which is the ratio of the flux of a particular component *i* of the mixture to the mass transfer coefficient k_i. The mass transfer coefficient for a narrow gap configuration with only one permeable side is given as [46]

$$k_i = 0.589 \left(\frac{2vD_i^2}{hL}\right)^{1/3} \quad \text{Eq.8}$$

where D_i is the diffusion coefficient of the component *i* in the mixture, calculated according Lüdtke et al. [40], *v* is velocity in the cell and *L* is the cell radius . The rejection factor for CH_4 and CO_2 is 0.99 and 0.78, respectively. The calculated Peclet numbers for both gases have a value in the range of $0.5 \cdot 10^{-3}$ - $7 \cdot 10^{-3}$, hence the concentration polarization modulus equals *M*= 1 for all tested trans-membrane pressures. Therefore, we may safely conclude that concentration polarization is not significant for the conditions used for our measurements.

Another important consideration to make is that the N_2 sweeping gas is slightly less permeable than CH_4. Since the stage-cut of CH_4 is only 1.3-2% in our experiments at a pressure difference of 100 kPa (Table S4 and Table S5), the amount of N_2 diffusing in the opposite direction will be similar or lower. Therefore, the N_2 sweep gas will not affect the gas concentrations at either side of the membrane significantly, and thus perturb the overall mass balance and the permeability calculations.

3.2 Effect of aging and membrane conditioning

At the end of the entire measurement cycle using different mixtures, the effect of long-term exposure of the membrane to CO_2 was studied by permeation tests of both pure gases (CO_2 and CH_4). For this study, the membrane was exposed to pure CO_2 at 25 °C and 500 kPa inside the closed permeation cell for two weeks. This is the approximately the same pressure as the CO_2 partial pressure in a CO_2/CH_4 mixture with 35% CO_2 at a pressure of 1500 kPa, in the typical

range for industrial biogas separation and may be indicative for the performance of the membrane under constant long-term operation. The results of these measurements, in comparison with those of the fresh membrane, are plotted in Fig. 6 and are also shown in the Robeson plot in Fig 4. Remarkably, the repeated pure gas permeation measurement showed a substantially higher ideal selectivity, mainly due to a decrease in the methane permeability at nearly constant CO_2 permeability.

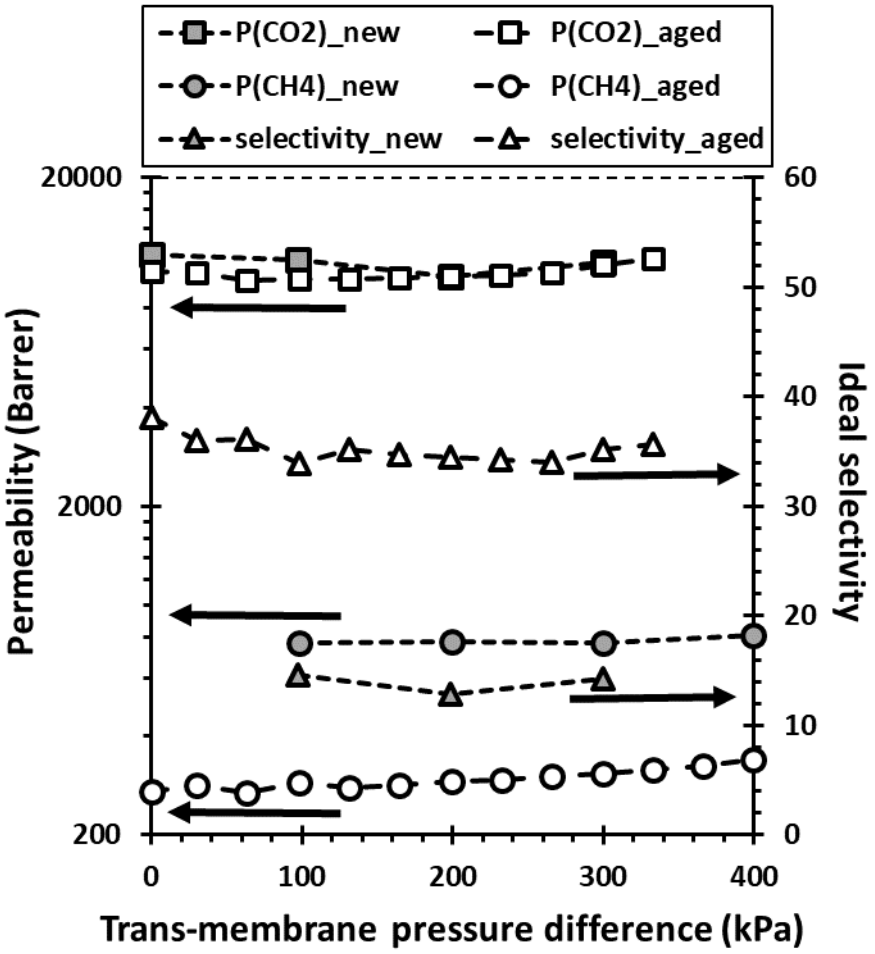

Fig. 6. Pure gas permeability and ideal selectivity for a freshly prepared membrane and for an aged membrane after exposure of the membrane to pure CO_2 for two weeks inside the permeation cell.

In contrast to what was seen for the gas mixtures, the permeability of pure gases remains almost constant with increasing partial pressure difference (Fig. 6, grey squares and grey circles) and also the selectivity remains constant (grey triangles). This suggests that the pressure-dependence of the mixed gas separation performance must be ascribed to a coupling effect.

While the CO_2 permeability remains nearly the same (Fig. 6, open squares), the ideal selectivity in the repeated measurement (open triangles) increases more than twofold because of a strongly

decreased permeability of CH_4 (open circles). The data are close to the 2019 upper bound for single dry gases with a similar selectivity but a much higher permeability as compared to PIM-2, recently reported by Fuoco *et al.* [47] The latter, presumably due to its hydrophobic nature, proved insensitive to the presence of humidity in the gas stream, contrary to what was observed for instance with PIM-1 when used for flue gas treatment [30].

We attribute the unusual increase in selectivity of PIM-TMN-Trip to simultaneous aging and dilation, which facilitates rearrangement of the polymer chains due to the high concentration of CO_2. This affects mainly the permeability of CH_4, probably by the formation of tighter bottle-necks between adjacent free volume elements but without a significant decrease of the total free volume, occupied by CO_2, and thus without a significant reduction of the permeability of CO_2. Such bottle-necks cannot be measured experimentally, because experimental techniques for analysis of the free volume all measure some kind of average, based on assumptions on the void shape and polymer-probe interactions [48] but they can be visualized by molecular modelling of the polymer structure. We have previously hypothesized, based on a model of PIM-MP-TB, [49] that such bottle-necks are responsible for the size-selectivity of PIMs.[50] The higher selectivity and constant CO_2 permeability differs from the previously observed physical ageing of PIM-TMN-Trip under ambient conditions, where both CO_2 and CH_4 permeability decrease [29], mainly as a result of reduced diffusivity and accompanied by increased size-selectivity [50]. The difference results from the fact that the membrane was left in a pressurized CO_2 environment, and thus in a swollen state, in contrast with the previous work where common physical ageing took place under mostly ambient conditions between subsequent measurements. This conditioning also differs from conventional CO_2-induced swelling and/or plasticisation at high CO_2 partial pressure, which results in an increase in the CH_4 permeation through the membrane, hence a decrease in selectivity [51]. A control experiment on a similar experimental setup (Fig S1, Ref. [S1-S3] under conditions of low stage cut and high feed flow rates shows that in an experimental run with a step-wise increase and decrease of the feed pressure some hysteresis occurs (Fig. 4, Fig. S2-S3). After a total run of 7 hours in the pressure range of 1-6 bar (CO_2 partial pressure 312 kPa), the permeability is slightly higher and the selectivity slightly lower than at the beginning of the experiment. This confirms that on a relatively short time scale the exposure to CO_2 only leads to dilation of the polymer. The latter is also typical for polymers with lower free volume, where CO_2 exposure always leads to relatively strong dilation, and a consequently lower selectivity [52], unless the polymer is cross-linked and strong dilation is inhibited [53]. Instead, in PIMs a much larger fraction of the gas is absorbed inside the already available free volume and the effect of competitive sorption might be as important as that of dilation or plasticization. The unusual increase in selectivity upon aging with CO_2 is remarkably similar that found in by work of Yampolskii et al., where the membrane was aged (without CO_2 exposure) inside the permeation cell under strained conditions [54]. Polyetherimide membranes with a small amount of residual solvent were found to increase their selectivity significantly if aged under strained conditions due to a combination of aging and loss of residual solvent, resulting also in an increase in the density of the samples. The effect of the strain was that the polymer could not relax equally in

all dimensions, and this led to a relatively large decrease in permeability of for instance N_2 with respect to O_2.

After the complete measurement cycle, the membrane was soaked in methanol for 24h and then dried in a stream of nitrogen for over 24 hours to test if the structural changes could be either reversed or improved. Bernardo et al. showed for PIM-1 that soaking in alcohol restores almost completely the original permeability of a membrane before ageing [55]Unfortunately, it was found that the used membrane had crazed under the pressure of the O-ring, which led to the formation of pinhole defects. We attribute the crazing to swelling of the membrane in MeOH and the subsequent shrinkage upon drying but also to stresses accumulated in the membrane during the various pressurizing and depressurizing steps. Therefore, this control experiment could not be performed. It must be noted that this procedure is not only fundamentally different from the time lag method in terms of the measurement principle, but it is also different in terms of the membrane conditioning because it does not require an evacuation step. We have shown previously that the initial vacuum on a PIM membrane may cause irreversible changes in the permeability (Fig. 5 in [56]). Besides the instantaneous change, the first vacuum on a freshly prepared membrane also seems to 'trigger' a faster aging process [57] probably because of a slight collapse of the free volume when the last traces of adsorbed species are removed. This may in part explain the different ageing behaviour.

3.3 Comparison with the state of the art

A comparison of our membrane with the results of other PIM membranes from the literature is shown in Fig. 7, including the data of PIM-TMN-Trip membrane measured by Rose et al. [21]. It may be concluded that our experiments yielded a lower permeability and selectivity for the freshly MeOH-soaked membrane than the reported values (likely due to the different method of permeability measurement and to the different boundary conditions) but it follows the trend of other PIMs. As for the CO_2 treated membrane, the increased selectivity moved the membrane performance above the Robeson upper bound, which defines the limit of what could be expected for PIM membranes. This behaviour deserves further attention to confirm that CO_2 can be used to tailor the permeability and to stabilize membrane aging, analogous to the technique described by Scholes et al. [58]. Alternatively, this treatment could be used for a rejuvenation process, which Yi et al. [28] attribute to the removal of a highly sorbing feed component.

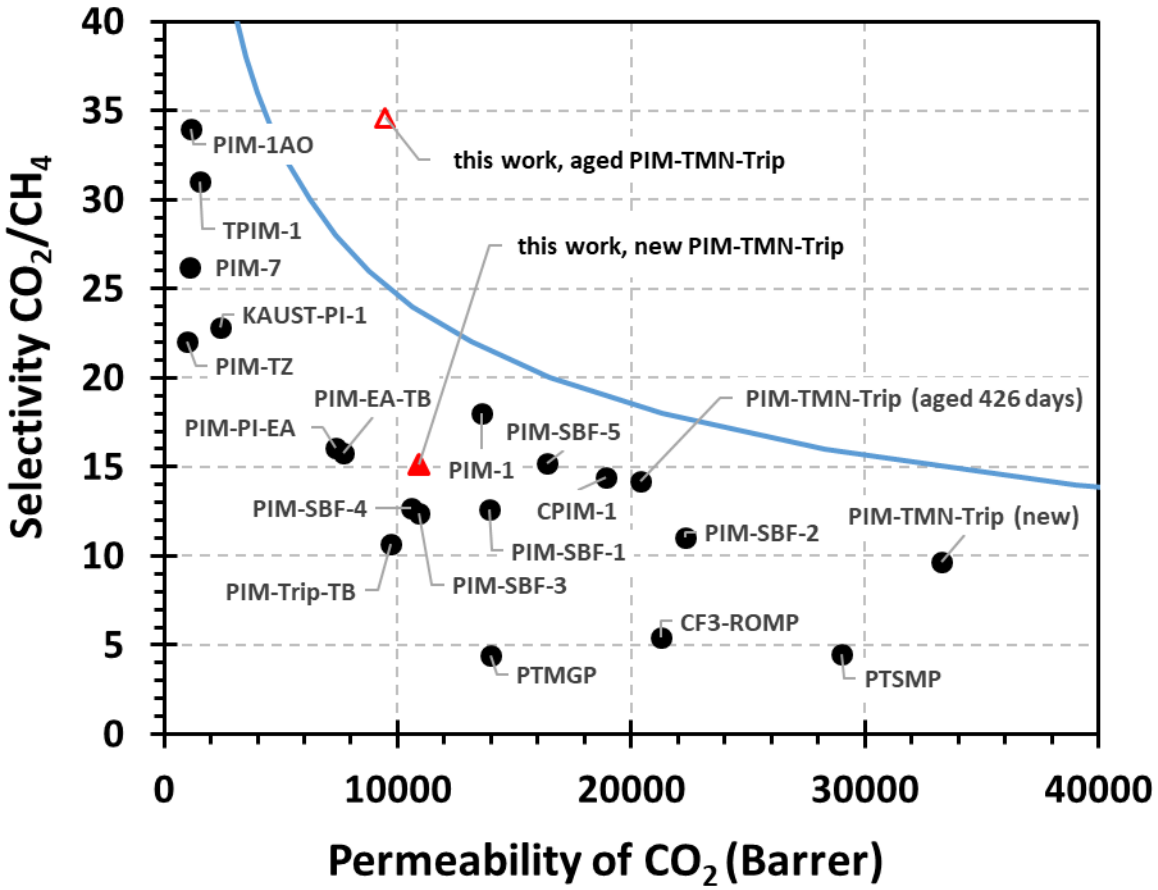

Fig. 7. Trade-off diagram between selectivity and permeability diagram for CO_2/CH_4 with compilation of result for polymers with intrinsic microporosity from the literature [29] for ideal selectivity. Blue line indicate 2019 upper bound by Comesaña-Gándara *et al*. [29]

4 Conclusions

PIM-TMN-Trip membranes show excellent separation properties for model mixtures of CO_2/CH_4 and for real biogas at small pressure difference, with performance lying between the 2008 and the recently defined 2019 CO_2/CH_4 upper bounds for pure gases. With increasing upstream pressure, the permeability of CO_2 decreased, as well as the mixed gas selectivity, whereas the ideal selectivity remained constant. For CO_2 permeability of pure gas, pristine membranes had a permeability of around $10 \cdot 10^3$ Barrer with an ideal selectivity of about 15. Interestingly, CO_2 treatment at 5 bar strongly enhances the ideal selectivity to values in the range of 34-39 without reducing the CO_2 permeability due to ageing in a swollen state. This condition may be representative for long-term operation of the membrane (e.g. 15 bar with 35% CO_2 in the feed gas), and the data show that even a 10 µm thick film has a high enough CO_2 permeability (>1000 GPU) to have potential as a commercial membrane. The presence of over 400 ppm of H_2S in the raw biogas does not affect the membrane transport and separation

properties significantly, opening interesting perspectives for the use of this membrane in raw biogas separation without the need of thorough pre-treatment.

Acknowledgements

Research on biogas upgrading presented in this work was supported by EU structural funding in the frame of Operational Programme Research, Development and Education, project No. CZ.02.1.01./0.0/0.0/17_049/0008419 „COOPERATION“.

References

[1] Forest bioenergy, carbon capture and storage, and carbon dioxide removal: an update., in: EASAC Reports, European Academies Science Advisory Council, 2019.

[2] S. Heile, S. Rosenberger, A. Parker, B. Jefferson, E.J. McAdam, Establishing the suitability of symmetric ultrathin wall polydimethylsiloxane hollow-fibre membrane contactors for enhanced CO2 separation during biogas upgrading, Journal of Membrane Science, 452 (2014) 37-45.

[3] X.Y. Chen, H. Vinh-Thang, A.A. Ramirez, D. Rodrigue, S. Kaliaguine, Membrane gas separation technologies for biogas upgrading, RSC Adv., 5 (2015) 24399-24448.

[4] Y.W. Jeon, D.H. Lee, Gas Membranes for CO2/CH4 (Biogas) Separation: A Review, Environ. Eng. Sci., 32 (2015) 71-85.

[5] J. Tao, J.L. Wang, L.Y. Zhu, X. Chen, Integrated design of multi-stage membrane separation for landfill gas with uncertain feed, Journal of Membrane Science, 590 (2019) 17.

[6] G. Sethunga, J. Lee, R. Wang, T.H. Bae, Influence of membrane characteristics and operating parameters on transport properties of dissolved methane in a hollow fiber membrane contactor for biogas recovery from anaerobic effluents, Journal of Membrane Science, 589 (2019) 13.

[7] E. Esposito, L. Dellamuzia, U. Moretti, A. Fuoco, L. Giorno, J.C. Jansen, Simultaneous production of biomethane and food grade CO2 from biogas: an industrial case study, Energy & Environmental Science, 12 (2019) 281-289.

[8] M. Karaszova, Z. Sedlakova, P. Izak, Gas permeation processes in biogas upgrading: A short review, Chem Pap, 69 (2015) 1277-1283.

[9] D.F. Sanders, Z.P. Smith, R. Guo, L.M. Robeson, J.E. McGrath, D.R. Paul, B.D. Freeman, Energy-efficient polymeric gas separation membranes for a sustainable future: A review, Polymer, 54 (2013) 4729-4761.

[10] M.T. Ho, G.W. Allinson, D.E. Wiley, Reducing the cost of CO2 capture from flue gases using membrane technology, Ind Eng Chem Res, 47 (2008) 1562-1568.

[11] E. Favre, R. Bounaceur, D. Roizard, Biogas, membranes and carbon dioxide capture, J Membrane Sci, 328 (2009) 11-14.

[12] M. Scholz, T. Melin, M. Wessling, Transforming biogas into biomethane using membrane technology, Renewable & Sustainable Energy Reviews, 17 (2013) 199-212.

[13] C.Y. Chuah, K. Goh, Y. Yang, H. Gong, W. Li, H.E. Karahan, M.D. Guiver, R. Wang, T.H. Bae, Harnessing Filler Materials for Enhancing Biogas Separation Membranes, Chem Rev, 118 (2018) 8655-8769.

[14] I. Borisov, D. Bakhtin, Jose M. Luque-Alled, A. Rybakova, V. Makarova, A.B. Foster, W.J. Harrison, V. Volkov, V. Polevaya, P. Gorgojo, E. Prestat, P.M. Budd, A. Volkov, Synergistic enhancement of gas selectivity in thin film composite membranes of PIM-1, Journal of Materials Chemistry A, 7 (2019) 6417-6430.

[15] R.S. Bhavsar, T. Mitra, D.J. Adams, A.I. Cooper, P.M. Budd, Ultrahigh-permeance PIM-1 based thin film nanocomposite membranes on PAN supports for CO2 separation, J Membrane Sci, 564 (2018) 878-886.
[16] M.M. Khan, V. Filiz, T. Emmler, V. Abetz, T. Koschine, K. Ratzke, F. Faupel, W. Egger, L. Ravelli, Free volume and gas permeation in anthracene maleimide-based polymers of intrinsic microporosity, Membranes (Basel), 5 (2015) 214-227.
[17] P. Bernardo, V. Scorzafave, G. Clarizia, E. Tocci, J.C. Jansen, A. Borgogno, R. Malpass-Evans, N.B. McKeown, M. Carta, F. Tasselli, Thin film composite membranes based on a polymer of intrinsic microporosity derived from Troger's base: A combined experimental and computational investigation of the role of residual casting solvent, J Membrane Sci, 569 (2019) 17-31.
[18] J. Benito, J. Vidal, J. Sanchez-Lainez, B. Zornoza, C. Tellez, S. Martin, K.J. Msayib, B. Comesana-Gandara, N.B. McKeown, J. Coronas, I. Gascon, The fabrication of ultrathin films and their gas separation performance from polymers of intrinsic microporosity with two-dimensional (2D) and three-dimensional (3D) chain conformations, J Colloid Interface Sci, 536 (2019) 474-482.
[19] C.G. Bezzu, M. Carta, M.-C. Ferrari, J.C. Jansen, M. Monteleone, E. Esposito, A. Fuoco, K. Hart, T.P. Liyana-Arachchi, C.M. Colina, N.B. McKeown, The synthesis, chain-packing simulation and long-term gas permeability of highly selective spirobifluorene-based polymers of intrinsic microporosity, Journal of Materials Chemistry A, 6 (2018) 10507-10514.
[20] A. Fuoco, B. Comesana-Gandara, M. Longo, E. Esposito, M. Monteleone, I. Rose, C.G. Bezzu, M. Carta, N.B. McKeown, J.C. Jansen, Temperature Dependence of Gas Permeation and Diffusion in Triptycene-Based Ultrapermeable Polymers of Intrinsic Microporosity, ACS Appl Mater Interfaces, 10 (2018) 36475-36482.
[21] I. Rose, C.G. Bezzu, M. Carta, B. Comesana-Gandara, E. Lasseuguette, M.C. Ferrari, P. Bernardo, G. Clarizia, A. Fuoco, J.C. Jansen, K.E. Hart, T.P. Liyana-Arachchi, C.M. Colina, N.B. McKeown, Polymer ultrapermeability from the inefficient packing of 2D chains, Nat Mater, 16 (2017) 932-937.
[22] I. Rose, M. Carta, R. Malpass-Evans, M.-C. Ferrari, P. Bernardo, G. Clarizia, J.C. Jansen, N.B. McKeown, Highly Permeable Benzotriptycene-Based Polymer of Intrinsic Microporosity, ACS Macro Letters, 4 (2015) 912-915.
[23] I. Hossain, S.Y. Nam, C. Rizzuto, G. Barbieri, E. Tocci, T.-H. Kim, PIM-polyimide multiblock copolymer-based membranes with enhanced CO2 separation performances, J Membrane Sci, 574 (2019) 270-281.
[24] Y. Wang, X. Ma, B.S. Ghanem, F. Alghunaimi, I. Pinnau, Y. Han, Polymers of intrinsic microporosity for energy-intensive membrane-based gas separations, Materials Today Nano, 3 (2018) 69-95.
[25] C. Ma, J.J. Urban, Polymers of Intrinsic Microporosity (PIMs) Gas Separation Membranes: A mini Review, Proceedings of the Nature Research Society, 2 (2018).
[26] Z.X. Low, P.M. Budd, N.B. McKeown, D.A. Patterson, Gas Permeation Properties, Physical Aging, and Its Mitigation in High Free Volume Glassy Polymers, Chem Rev, 118 (2018) 5871-5911.
[27] M.L. Jue, R.P. Lively, Targeted gas separations through polymer membrane functionalization, Reactive and Functional Polymers, 86 (2015) 88-110.
[28] S. Yi, B. Ghanem, Y. Liu, I. Pinnau, W.J. Koros, Ultraselective glassy polymer membranes with unprecedented performance for energy-efficient sour gas separation, Sci Adv, 5 (2019) eaaw5459.
[29] B. Comesaña-Gándara, J. Chen, C.G. Bezzu, M. Carta, I. Rose, M.-C. Ferrari, E. Esposito, A. Fuoco, J.C. Jansen, N.B. McKeown, Redefining the Robeson upper bounds for CO2/CH4 and CO2/N2 separations using a series of ultrapermeable benzotriptycene-based polymers of intrinsic microporosity, Energy & Environmental Science, (2019).
[30] E. Lasseuguette, M. Carta, S. Brandani, M.-C. Ferrari, Effect of humidity and flue gas impurities on CO2 permeation of a polymer of intrinsic microporosity for post-combustion capture, Int J Greenh Gas Con, 50 (2016) 93-99.

[31] P. Stanovsky, A. Zitkova, M. Karaszova, M. Šyc, J. Carolus Jansen, B. Comesaña Gándara, N. McKeown, P. Izak, Flue gas purification with membranes based on the polymer of intrinsic microporosity PIM-TMN-Trip, Separation and Purification Technology, 25 (2020) 9-15.
[32] M. Kárászová, Friess, K., Šípek, M., Jansen, J. C., Izák, P., Biogas upgrading for the 21st century, in: I.C. R. Litonjua (Ed.) Biogas: Production, consumption and applications, Nova Science Publishers, New York, NY, USA, 2011, pp. 91-116.
[33] L.M. Robeson, The upper bound revisited, J Membrane Sci, 320 (2008) 390-400.
[34] G. Genduso, Y. Wang, B.S. Ghanem, I. Pinnau, Permeation, sorption, and diffusion of CO2-CH4 mixtures in polymers of intrinsic microporosity: The effect of intrachain rigidity on plasticization resistance, J Membrane Sci, 584 (2019) 100-109.
[35] G. Genduso, B.S. Ghanem, I. Pinnau, Experimental Mixed-Gas Permeability, Sorption and Diffusion of CO(2)-CH(4) Mixtures in 6FDA-mPDA Polyimide Membrane: Unveiling the Effect of Competitive Sorption on Permeability Selectivity, Membranes (Basel), 9 (2019).
[36] C. Scholes, S. Kentish, G. Stevens, Effects of Minor Components in Carbon Dioxide Capture Using Polymeric Gas Separation Membranes, Sep Purif Rev, 38 (2009) 1-44.
[37] C.A. Scholes, G.W. Stevens, S.E. Kentish, The effect of hydrogen sulfide, carbon monoxide and water on the performance of a PDMS membrane in carbon dioxide/nitrogen separation, J Membrane Sci, 350 (2010) 189-199.
[38] C.A. Scholes, G.W. Stevens, S.E. Kentish, Permeation through CO2selective glassy polymeric membranes in the presence of hydrogen sulfide, Aiche J, 58 (2012) 967-973.
[39] D.R.Y. Paul, Y. P., Polymeric Gas Separation Membranes, 1st ed., CRC Press Boca Raton 1994.
[40] O. Ludtke, R.D. Behling, K. Ohlrogge, Concentration polarization in gas permeation, J Membrane Sci, 146 (1998) 145-157.
[41] E. Nagy, R. Nagy, J. Dudas, Separate Expression of Polarization Modulus and Enrichment by Mass Transport Parameters for Membrane Gas Separation, Industrial & Engineering Chemistry Research, 52 (2013) 10441-10449.
[42] Z.F. Cui, Y. Jiang, R.W. Field, Chapter 1 - Fundamentals of Pressure-Driven Membrane Separation Processes, in: Z.F. Cui, H.S. Muralidhara (Eds.) Membrane Technology, Butterworth-Heinemann, Oxford, 2010, pp. 1-18.
[43] P. Luis, Chapter 1 - Introduction, in: P. Luis (Ed.) Fundamental Modelling of Membrane Systems, Elsevier, 2018, pp. 1-23.
[44] E. Nagy, Chapter 18 - Membrane Gas Separation, in: E. Nagy (Ed.) Basic Equations of Mass Transport Through a Membrane Layer (Second Edition), Elsevier, 2019, pp. 457-481.
[45] P.A. Schweitzer, Handbook of Separation Techniques for Chemical Engineers, McGraw-Hill Book Company, New York, 1979.
[46] P.C. Wankat, Rate-controlled separations, Elsevier Science Publishers, New York, 1990.
[47] A. Fuoco, B. Satilmis, T. Uyar, M. Monteleone, E. Esposito, C. Muzzi, E. Tocci, M. Longo, M.P. De Santo, M. Lanč, K. Friess, O. Vopička, P. Izák, J.C. Jansen, Comparison of pure and mixed gas permeation of the highly fluorinated polymer of intrinsic microporosity PIM-2 under dry and humid conditions: Experiment and modelling, J Membrane Sci, 594 (2020).
[48] J.C. Jansen, M. Macchione, E. Tocci, L. De Lorenzo, Y.P. Yampolskii, O. Sanfirova, V.P. Shantarovich, M. Heuchel, D. Hofmann, E. Drioli, Comparative Study of Different Probing Techniques for the Analysis of the Free Volume Distribution in Amorphous Glassy Perfluoropolymers, Macromolecules, 42 (2009) 7589-7604.
[49] R. Williams, L.A. Burt, E. Esposito, J.C. Jansen, E. Tocci, C. Rizzuto, M. Lanc, M. Carta, N.B. McKeown, A highly rigid and gas selective methanopentacene-based polymer of intrinsic microporosity derived from Troger's base polymerization, Journal of Materials Chemistry A, 6 (2018) 5661-5667.
[50] A. Fuoco, C. Rizzuto, E. Tocci, M. Monteleone, E. Esposito, P.M. Budd, M. Carta, B. Comesaña-Gándara, N.B. McKeown, J.C. Jansen, The origin of size-selective gas transport through polymers of intrinsic microporosity, Journal of Materials Chemistry A, 7 (2019) 20121-20126.

[51] A. Bos, I.G.M. Pünt, M. Wessling, H. Strathmann, CO2-induced plasticization phenomena in glassy polymers, J Membrane Sci, 155 (1999) 67-78.
[52] J. Kim, W. Koros, D. Paul, Effects of CO2 exposure and physical aging on the gas permeability of thin 6FDA-based polyimide membranes Part 1. Without crosslinking, J Membrane Sci, 282 (2006) 21-31.
[53] J. Kim, W. Koros, D. Paul, Effects of CO2 exposure and physical aging on the gas permeability of thin 6FDA-based polyimide membranes Part 2. with crosslinking, J Membrane Sci, 282 (2006) 32-43.
[54] Y. Yampolskii, A. Alentiev, G. Bondarenko, Y. Kostina, M. Heuchel, Intermolecular Interactions: New Way to Govern Transport Properties of Membrane Materials, Ind Eng Chem Res, 49 (2010) 12031-12037.
[55] P. Bernardo, E. Bazzarelli, F. Tasselli, G. Clarizia, C.R. Mason, L. Maynard-Atem, P.M. Budd, M. Lanc, K. Pilnacek, O. Vopicka, K. Friess, D. Fritsch, Y.P. Yampolskii, V. Shantarovich, J.C. Jansen, Effect of physical aging on the gas transport and sorption in PIM-1 membranes, Polymer, 113 (2017) 283-294.
[56] E. Tocci, L. De Lorenzo, P. Bernardo, G. Clarizia, F. Bazzarelli, N.B. McKeown, M. Carta, R. Malpass-Evans, K. Friess, K. Pilnáček, M. Lanč, Y.P. Yampolskii, L. Strarannikova, V. Shantarovich, M. Mauri, J.C. Jansen, Molecular Modeling and Gas Permeation Properties of a Polymer of Intrinsic Microporosity Composed of Ethanoanthracene and Tröger's Base Units, Macromolecules, 47 (2014) 7900-7916.
[57] M. Longo, M.P. De Santo, E. Esposito, A. Fuoco, M. Monteleone, L. Giorno, B. Comesaña-Gándara, J. Chen, C.G. Bezzu, M. Carta, I. Rose, N.B. McKeown, J.C. Jansen, Correlating Gas Permeability and Young's Modulus during the Physical Aging of Polymers of Intrinsic Microporosity Using Atomic Force Microscopy, Ind Eng Chem Res, 59 (2019) 5381-5391.
[58] C.A. Scholes, S. Kanehashi, Polymer of Intrinsic Microporosity (PIM-1) Membranes Treated with Supercritical CO(2), Membranes (Basel), 9 (2019).